Marine Environmental Research 200 (2024) 106649

Contents lists available at ScienceDirect

Marine Environmental Research

journal homepage: www.elsevier.com/locate/marenvrev

Vertical distributions of megafauna on inactive vent sulfide features correspond to their feeding modes

Michael J. Meneses [a], Stace E. Beaulieu [a], Ayinde C. Best [a,b], Lauren N. Dykman [a,c], Susan W. Mills [a], Jyun-Nai Wu [d], Lauren S. Mullineaux [a,*]

[a] Woods Hole Oceanographic Institution, 266 Woods Hole Rd, Woods Hole, MA, 02540, USA
[b] Wheaton College, 26 E Main St, Norton, MA, 02766, USA
[c] University of Victoria, 3800 Finnerty Rd, Victoria, BC, V8P 5C2, Canada
[d] Scripps Institution of Oceanography, 9500 Gilman Drive, La Jolla, CA, 92093, USA

A B S T R A C T

The discovery of inactive hydrothermal vent sulfide features near 9°50′N on the East Pacific Rise provides an opportunity to investigate the distribution and feeding ecology of communities inhabiting this type of habitat. We quantify megafaunal distributions on two features, Lucky's Mound and Sentry Spire, to determine how taxonomic composition and feeding traits vary with vertical elevation. Fifty-one morphotypes, categorized by feeding mode, were identified from three levels of the features (spire, apron, and base) and the surrounding flat oceanic rise. About half of the morphotypes (26 of 51) were only observed at the sulfide features. Passive suspension feeders were more abundant on the spires, where horizontal particulate flux is expected to be elevated, than the base or rise. Deposit feeders tended to be more abundant on the base and rise, where deposition is expected to be enhanced, but were unexpectedly abundant higher up on Sentry Spire. Community differences between the two sulfide features suggest that other processes, such as feature-specific chemoautotrophic production, may also influence distributions.

1. Introduction

Deep-sea hydrothermal vents are benthic habitats that occur in geologically active regions of the seafloor, such as mid-ocean ridges and back-arc basins. Active hydrothermal vents release hot metal- and sulfide-rich fluids from beneath the seafloor into the surrounding water. This mixing causes metallic sulfides to precipitate out of the fluid leading to the formation of vent structures such as chimneys and accumulating as mineral deposits over time (Goldfarb et al., 1983; Tivey 2007). After venting ceases, the temperature and hydrogen sulfide levels decrease to levels of ambient deep seawater and the inactive sulfide features develop different structural, chemical, and environmental conditions, making them a distinct habitat (Erickson et al., 2009; Orcutt et al., 2020). Inactive sulfide deposits tend to be small, spanning tens of meters on the seafloor, and widely spaced (Hannington et al., 2010), but can persist for thousands of years after venting has ceased (Jamieson and Gartman 2020).

Imaging studies of these features suggest that they may provide habitat heterogeneity and increased niche space for benthic organisms. The megafauna (animals visible in seafloor images, typically centimeter scale or larger) inhabiting inactive sulfides appear to be non-endemic species that are observed in other habitats in the deep sea (Boschen et al., 2013; Van Dover 2019). Analyses of their community structure, however, indicate that relative abundances and co-occurrences of taxa differ from assemblages on active vents and the surrounding seafloor (Boschen et al., 2015; Gerdes et al., 2019, 2021; Neufeld et al., 2022). Although no megafauna have been classified as endemic to inactive sulfides, several smaller taxa (macrofauna) have been reported only from sulfide features: the polychaete *Eunoe alvinella*, (Pettibone, 1984) two species of the polychaete *Amphisamytha* (Zhou et al., 2019), and multiple species of the gastropods *Neolepetopsis* (McLean 1990; Chen et al., 2021) and *Melanodrymia* (Chen et al., 2024).

Numerous processes influence the community composition in deep-sea environments and several are particularly relevant to inactive sulfide features as they may result in distinct megafaunal assemblages. High abundances of benthic organisms, especially suspension feeders, are often found on hard substrata with topographic relief, likely due to increased flux of particulate organic food in enhanced currents (Leichter and Witman 1997). Boschen et al. (2015) postulate that the hard substratum provided by inactive sulfide deposits facilitates attachment of taxa such as sponges, hydroids, corals and anemones, which, in their study, were uncommon on the surrounding sedimented seafloor. Populations on inactive features may also benefit from chemoautotrophic production arriving in particulate form from nearby active vent

* Corresponding author.
E-mail address: lmullineaux@whoi.edu (L.S. Mullineaux).

https://doi.org/10.1016/j.marenvres.2024.106649
Received 17 May 2024; Received in revised form 5 July 2024; Accepted 16 July 2024
Available online 16 July 2024

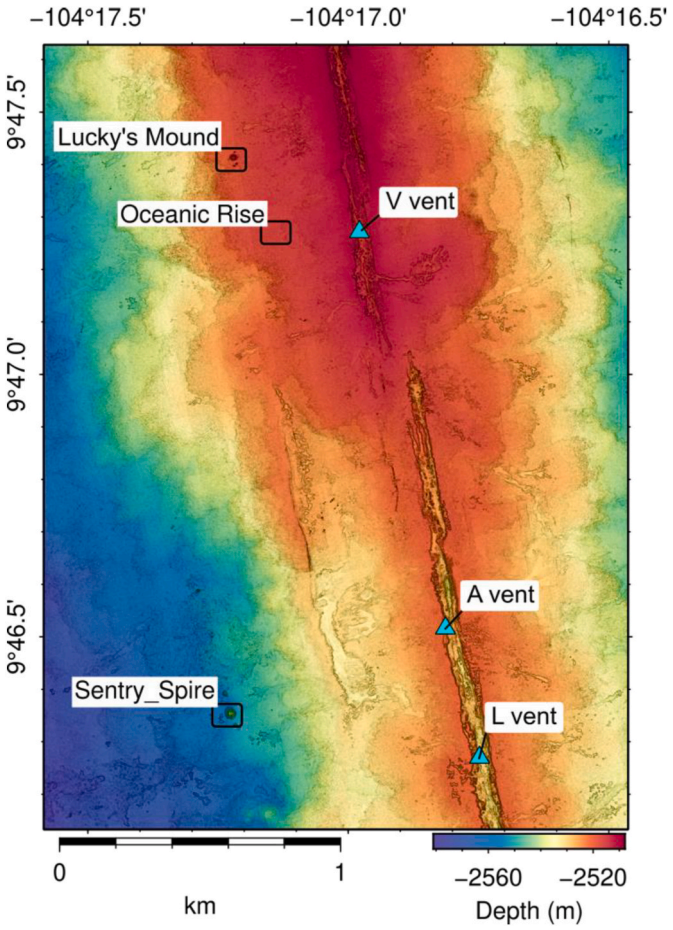

Fig. 1. Locations of study sites west of the axial valley near 9°50′N on the East Pacific Rise. Lucky's Mound and Sentry Spire are inactive sulfide features and the Oceanic Rise is a nearby flat area for comparison. Locations of active vents V, A, and L are noted on the axial valley. Bathymetric data from Parnell-Turner et al. (2021).

communities (Erickson et al., 2009). Alternatively, rock-based chemoautotrophic production by microbes on the inactive sulfide feature itself, as reported by Kato et al. (2010) and more recently by Achberger et al. (2024), may contribute to the nutrition of animals living there.

In the present study, we investigate the megafaunal taxa on two newly discovered inactive sulfide features (Lucky's Mound and Sentry Spire) near the East Pacific Rise (EPR) 9°50′N vent field (Fig. 1), with a focus on the potential for vertical position on the feature (Fig. 2) and the associated patterns in organic particle flux and deposition, to influence faunal abundance and distribution. We characterize feeding modes for the taxa to gain insight into how organisms with similar modes may be influenced by environmental conditions (Cadotte et al., 2011; Mouillot et al., 2013). For passive suspension feeders and deposit feeders, food availability is expected to vary with position on the sulfide feature; i.e., suspended organic particulate flux for suspension feeders is likely to be enhanced near top-most, prominent spire(s) where currents are intensified, whereas deposition of organic particles and carrion is likely to be enhanced near the base where the substratum is nearly horizontal. Active suspension feeders may be less dependent on current-mediated particle flux because they create their own feeding currents. A correspondence between feeding modes and position on the sulfide feature would provide a mechanistic explanation for the presence of distinctly different, but not endemic, assemblages on these features. However, an influence of chemoautotrophic production, local or transported, cannot be discounted by an imaging study such as ours, so a faunal comparison between two features of different sizes and distances from active vents may provide insight into whether local topographic influences dominate. In addition to ecological insight, our study contributes to the growing recognition of biodiversity associated with inactive sulfide deposits, a resource under consideration for deep-sea mining in other regions.

2. Methods

2.1. Study sites

The EPR 9°50′N hydrothermal vent field is located on a segment of the ridge whose geology, chemistry and biology have been studied for over 40 years (Fornari et al., 2012). Despite this historical focus, recent near-bottom multibeam bathymetric studies with the autonomous underwater vehicle (AUV) *Sentry* have led to the new discovery of off-axis inactive sulfide features located hundreds of meters from the EPR axial valley (Wu et al., 2022; McDermott et al., 2022). The two inactive sulfides selected for megafaunal analysis in the present study are each composed of a central mound with chimney "spires", surrounded by a sloping "apron" with collapsed sulfide rubble and loose deposit, and a flatter "base" where the deposit intersects with the basalt seafloor. Lucky's Mound has a central mound ~30 m diameter, 12 m tall, with multiple inactive spires (Fig. 2a,d). Sentry Spire has a slightly larger central mound with a single large spire, 16 m tall, and two smaller features to the north and south (Fig. 2b,e). Topographic variation across the Oceanic Rise survey area was less than 1 m in height (Fig. 2c,f), whereas distinct projections of 2–3 m occur on the sulfide features.

2.2. Imaging surveys

Imaging surveys for this study were made during research expeditions on the RV *Atlantis* (AT42-21 in 2019) and RV *Roger Revelle* (RR2102 in 2021) to the 9°50′N region of the EPR. Seafloor images were captured with a downward-facing Model D3300 24-megapixel digital still camera mounted on the deep submergence vehicle *Alvin* in 2019 and the remotely operated vehicle *Jason II* in 2021. The camera captured images at 10-s intervals, in sync with a 300 Watt s^{-1}, high intensity strobe light. The camera was fitted with a Nikkor 20 mm f2.8 lens behind a domed optical port that produced a 38.6° × 55.7° field of view. Metadata associated with each image (coordinates, UTC timestamp, depth) were collected by the vehicles and processed on the ship after each dive.

Three separate surveys were conducted, two on inactive sulfide features and one on the nearby flat oceanic rise (Fig. 2). Lucky's Mound was opportunistically explored and surveyed in 2019 with a 60m × 60m grid that covered the central mound and some of the surrounding flat seafloor. Sentry Spire was surveyed in 2021 along three linear transects across the main spire, oriented roughly 120° apart. The oceanic rise was surveyed with a 60m × 60m grid at a similar seafloor depth to Lucky's Mound. Each survey was designed to cover a comparable area and habitat variation across the site. For the oceanic rise survey, the vehicle traveled at ~0.5 km h^{-1} at an altitude of ~5 m above the seafloor; this protocol was attempted on the inactive features, but with less precision due to difficulties in navigating the topography. In particular, the altitude for Sentry Spire images was often greater than 5 m. The seafloor resolution of images captured at 5 m altitude was 11.4 pixels cm^{-1} and the seafloor remained in focus up to 8 m altitude, corresponding to a resolution of 7.1 pixels cm^{-1}. Thus, megafaunal organisms as small as 3 cm in length, observed within 8 m of the camera lens, could be resolved for identification.

The topography of the inactive sulfide features required abrupt changes in the vehicle orientation and height that affected the quality of captured images. To ensure consistent quality of faunal data, images that were poorly illuminated or out of focus were removed from the study. Overlapping images were removed to prevent duplicate sampling. For each of the three surveys, the remaining transect images were randomly subsampled to a set of up to 50 images (49 for Lucky's Mound, 44 for

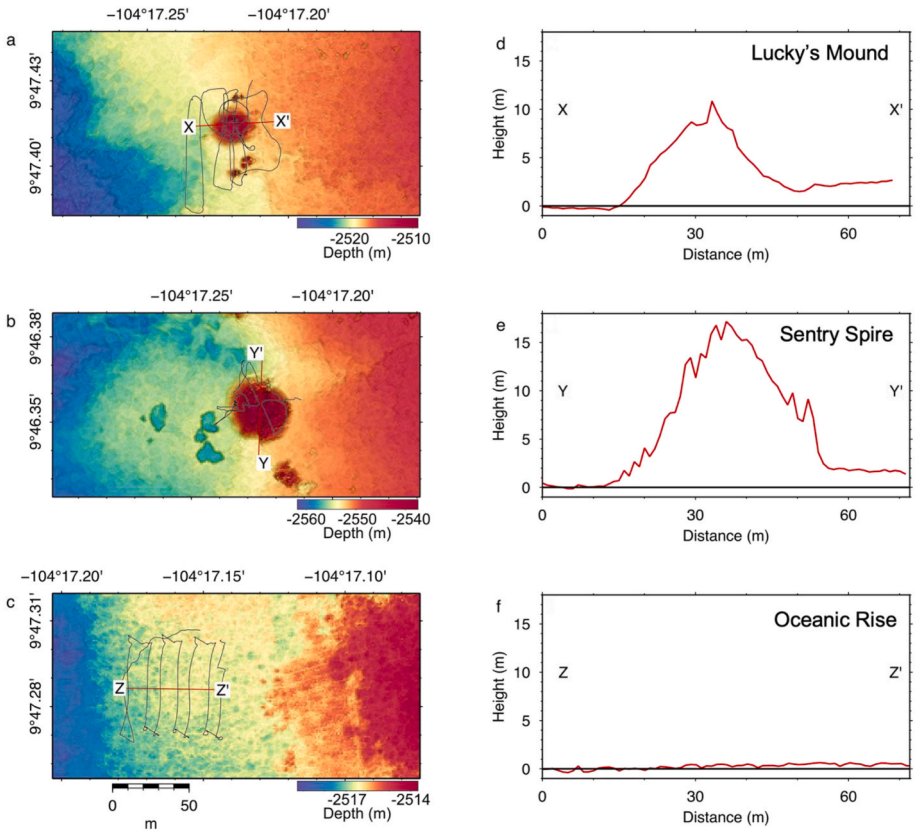

Fig. 2. Imaging survey paths (a–c) and vertical relief (d–f) from Lucky's Mound, Sentry Spire and nearby flat seafloor of the Oceanic Rise. Vertical relief shows height above bottom for each site from a cross-section (e.g., X-X′) across the highest point of the feature using GMT6 (Wessel et al., 2019).

Sentry Spire, and 50 for the oceanic rise) and annotated using the image processing software ImageJ (Schneider et al., 2012).

2.3. Image scaling and area corrections

The cameras did not have paired lasers for scale, so the camera altitude (m above seafloor) was used to estimate the total area of each image, as calculated from the camera field of view. In cases where topographic variation within an image caused portions to be > 8 m away from the camera, only the in-focus portions corresponding to an accurate altitude measurement (<8 m), were used for animal counts and area estimates. In occasional images of particularly complex topography, the vehicle's altitude measurement appeared inadequate for an accurate image scale. Rather than remove these images from analysis, we corrected the scale by using known sizes of megafaunal taxa. Ranges of typical animal sizes from the sulfide features were measured from images of galatheid squat lobsters (*Munidopsis*), unstalked crinoids (Antedonidae) and shrimp (Nematocarcinidae), selected from close-up, high-resolution (4K) videos of the study sites acquired with *Alvin* on a later cruise (AT50-06, December 2022). Beams from parallel lasers mounted 10 cm apart were visible in each screenshot and allowed for accurate measurement of those individuals using ImageJ. After measuring multiple (>5) individuals of each morphotype, a size range was calculated for use in assessing whether the scale for survey images containing these morphotypes was accurate, and adjusting the scale if necessary. For the few Sentry Spire images with questionable altitude measurements but no calibrated morphotypes in view, the areal scale was interpolated from the two nearest, reliably scaled, images. The typical area of an image was 18.50 m^2, corresponding to a camera altitude of 5 m, but areas in the full set of 143 images ranged from 3.37 to 47.37 m^2, due to variations in camera altitude and exclusions of regions that were out of focus.

Table 1
Feeding modes assigned to megafaunal morphotypes. Assignment is based on feeding traits reported for closely related taxa. The 'Unknown' mode contains only a single *Xenoturbella*-like morphotype. Descriptions modified from MarLIN (2006); 'Unknown' corresponds to 'Insufficient information'.

Feeding Mode	Description
Suspension Feeder	Organism captures particulate organic matter, including plankton, from the water column
Passive	Catching food on a filter or sticky apparatus held into flowing water
Active	Catching food on a filter by actively sweeping or pumping
Deposit Feeder	Organism which feeds on fragmented particulate matter on or within the substratum
Scavenger	Organism that actively feeds on dead animal matter
Predator	Organism that feeds by actively preying on other fauna, killing them for food
Grazer	Organism rasps microbial organisms from the substratum
Unknown	Feeding traits of related taxa are unknown

2.4. Megafauna and feeding modes

Benthic megafaunal (>3 cm) individuals that were clearly visible in images were counted and assigned a morphotype label, following common practice for visual-based surveys (Durden et al., 2016; Horton et al., 2021). Morphotypes were assigned to the lowest possible taxonomic level by referencing existing scientific literature, online databases, and expert opinions (Desbruyères et al., 2006; NOAA Ocean Exploration Benthic Deepwater Animal Identification Guide v3 2019; WoRMS Editorial Board 2022; Simon-Lledó et al., 2023). When morphotypes with similar appearance could not be distinguished reliably (e.g., various brittle stars), they were grouped together into a higher taxonomic level.

To infer how food type and availability influences the distribution of

Table 2
Density per 100 m^2 of 51 morphotypes in images from inactive sulfide features Lucky's Mound and Sentry Spire, and nearby flat Oceanic Rise. Densities are calculated from counts pooled over the total area of all images from each site: 49 images totaling 600.5 m^2 for Lucky's Mound, 44 images totaling 1148.1 m^2 for Sentry Spire, and 50 images totaling 905.9 m^2 for Oceanic Rise. Feeding modes assigned as described in Table 1.

Morphotype	Phylum	Feeding Mode	Lucky's Mound	Sentry Spire	Oceanic Rise
Xenophyophoroidea, cluster shaped	Foraminifera	Deposit	1.67	0	0.22
Xenophyophoroidea, dark	Foraminifera	Deposit	6.16	2.53	0.77
Xenophyophoroidea, white	Foraminifera	Deposit	5.66	5.05	17.22
Ctenophora Tentaculata	Ctenophora	Susp, Active	22.98	4.01	6.84
Hexactinellida Rossellidae	Porifera	Susp, Active	1.17	0.70	1.88
Hexactinellida, white leaf shaped	Porifera	Susp, Active	1.33	0	0.44
Hexactinellida, white spiked	Porifera	Susp, Active	0	1.57	0
Porifera, white round	Porifera	Susp, Active	0	0	0.11
Porifera, yellow round	Porifera	Susp, Active	1.33	0.44	0.33
Cladorhizidae	Porifera	Susp, Passive	0.67	4.53	0
Hydrozoa, medusa	Cnidaria	Predator	0.17	0	0
Actinaria, transparent	Cnidaria	Susp, Passive	0	0.61	0
Anthozoa, dark	Cnidaria	Susp, Passive	0	0	0.11
Octocorallia Anthomastus	Cnidaria	Susp, Passive	0	0.35	0
Octocorallia Primnoidae	Cnidaria	Susp, Passive	0	0	0.44
Octocorallia, Pennatulacea-like	Cnidaria	Susp, Passive	0.17	0	0
Cnidaria or Bryozoa	?Cnidaria	Susp, Passive	0	0.09	0
Xenoturbella-like	?Xenacoelomorpha	Unknown	8.16	0	0
Bryozoa, branched	Bryozoa	Susp, Active	0.33	0.09	0
Aphroditidae	Annelida	Predator	0.17	0	2.10
Polychaeta, blue bristled	Annelida	Predator	0.17	0	0
Polyplacophora, white chiton	Mollusca	Grazer	0	0.09	0
Vulcanoctopus hydrothermalis	Mollusca	Predator	0	0.09	0
Gastropoda, white	Mollusca	Scavenger	0.67	0	0
Bythograeidae, orange	Arthropoda	Scavenger	0	0	0.11
Colossendeidae	Arthropoda	Predator	0.33	0	0
Munidopsis	Arthropoda	Scavenger	5.00	1.22	0
Paguroidea	Arthropoda	Scavenger	0.33	0.09	0
Munnopsidae	Arthropoda	Scavenger	0.17	0.44	0.44
Nematocarcinidae	Arthropoda	Scavenger	22.81	4.79	3.75
Echinodermata or Cnidaria	?Echinodermata	Susp, Passive	0	0.26	0
Elasipodida, soft-spined	Echinodermata	Deposit	1.67	0.26	0.33
Holothuroidea, blue	Echinodermata	Deposit	0.33	0	0
Holothuroidea, brown	Echinodermata	Deposit	0.17	0	0.77
Holothuroidea, long-spined	Echinodermata	Deposit	1.50	0	0
Holothuroidea, pink	Echinodermata	Deposit	0	0.87	0.55
Holothuroidea, red	Echinodermata	Deposit	1.00	0.44	0.44
Holothuroidea, yellow	Echinodermata	Deposit	0.83	0.70	0.99
Asteroidea or Ophiuroidea	Echinodermata	Predator	0	0.26	0
Asteroidea, long-rayed white	Echinodermata	Predator	0	0.26	0
Asteroidea, orange	Echinodermata	Predator	0	0	0.11
Asteroidea, six-rayed white	Echinodermata	Predator	0.17	0	0
Ophiurida	Echinodermata	Scavenger	20.82	1.57	90.74
Antedonidae	Echinodermata	Susp, Passive	12.49	2.44	2.21
Bathycrinidae	Echinodermata	Susp, Passive	0.33	0.09	0.55
Brisingida, dark oral disc	Echinodermata	Susp, Passive	0.33	0	0
Brisingida, light oral disc	Echinodermata	Susp, Passive	0	0.17	0
Halosauridae	Chordata	Predator	0.50	0.26	0.11
Ophidiiformes, pointed pectoral fins	Chordata	Predator	0	0.09	0
Ophidiiformes, large head	Chordata	Predator	0	0.17	0.44
Ophidiiformes, zoarcid-like	Chordata	Predator	0.33	0.09	0

megafauna with different feeding strategies, each morphotype was categorized into one of seven different feeding modes, inferred from studies of closely related taxa as reported in textbooks and peer-reviewed literature. These assignments were cross-checked for consistency with existing trait databases, including recent functional trait studies focusing on hydrothermal vent fauna (Chapman et al., 2019; Dykman et al., 2021). Our feeding modes (Table 1) align to a "Characteristic feeding method" in the Biological Traits Information Catalogue (BIOTIC; MarLIN, 2006) and correspond to "Feeding Method/-Behaviour" in a recent review of trait-based approaches (Morim et al., 2023). Among the available trait types, we focused on feeding because of its potential association with organic food availability on abrupt topography, as in similar studies on benthic habitats (e.g., Boschen-Rose et al., 2021).

2.5. Analyses of megafaunal abundance and distribution

Patterns in community composition of morphotypes and feeding modes were compared between sites (Lucky's Mound, Sentry Spire, Oceanic Rise), and distributions of morphotypes and feeding modes were examined across vertical positions (base, apron, spire) at the two inactive sulfide features. Statistical analyses were performed using R version 4.2.3 (R Core Team 2023) unless otherwise noted.

For comparisons between sites, morphotype diversity was displayed using rarefaction curves as a function of number of individuals, which in this study are the total counts of individual megafauna in each multi-image survey. We also calculated Shannon diversity (Shannon 1948) and Pielou's evenness (Pielou 1966) for comparisons with other published findings. Counts of each morphotype were used to construct Bray-Curtis dissimilarity matrices (Bray and Curtis 1957) comparing community composition between study sites, and counts of each feeding mode were used similarly to compare functional composition. These

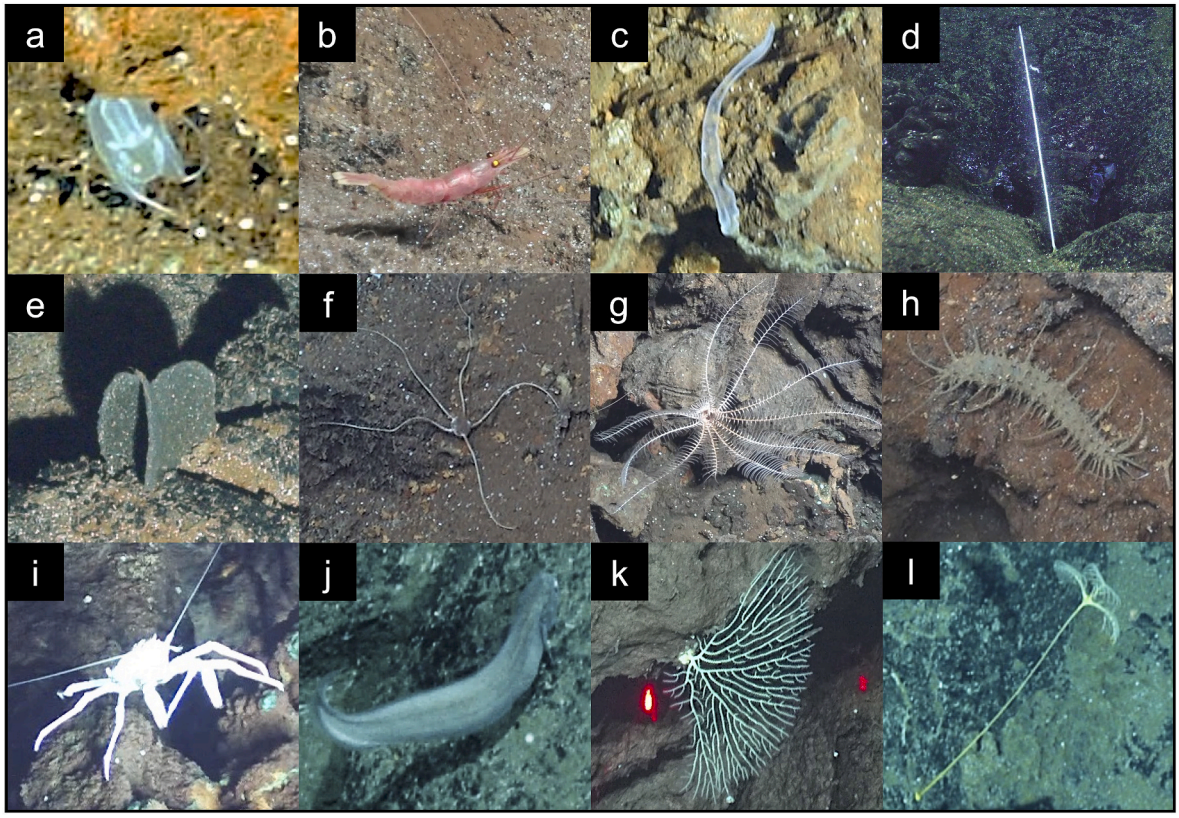

Fig. 3. Images of abundant or distinctive megafaunal morphotypes observed on sulfide features and the oceanic rise: (a) ctenophore, Tentaculata; (b) shrimp, Nematocarcinidae (c) *Xenoturbella*-like; (d) sponge, Cladorhizidae, e) dark xenophyophore, Xenophyophoroidea; (f) brittle star, Ophiurida; (g) crinoid, Antedonidae; (h) yellow holothurian, Holothuroidea; (i) squat lobster, *Munidopsis*; (j) fish, large-head Ophidiiformes; (k) branched bryozoan, Bryozoa; (l) crinoid, Bathycrinidae.

matrices were plotted as non-metric multidimensional scaling ordination plots to visualize differences between sites (Kruskal 1964). Permutational multivariate analysis of variance (PERMANOVA) and post-hoc pairwise comparisons were used to assess whether composition differences between sites were statistically significant (Anderson 2014). These analyses were conducted with functions rarecurve, diversity, metaMDS, and adonis2, in R package *vegan*, version 2.6–4 (Oksanen et al., 2022).

For comparisons across habitats on each sulfide feature, image locations were categorized into habitat types, according to position on the feature (spire, apron, and base). The oceanic rise (flat basalt seafloor) was categorized as a separate habitat. Counts and corrected area were used to calculate density (individuals m^{-2}) of morphotypes and feeding modes in each image and mean density for each habitat type. The statistical significance of differences in feeding-mode densities between habitats was assessed using a non-parametric Kruskal-Wallis test (Kruskal and Wallis 1952), as the condition of homogeneity of variance was not met for a one-way ANOVA. Post-hoc Dunn's comparison tests (Dunn 1961) were conducted using the R package *rstatix* version 0.7.2 (Kassambara 2023) to determine significant differences between habitats. Bonferroni corrections of p-values were used for the Kruskal-Wallis tests across five feeding modes, and for the Dunn's tests across the four habitat types (six comparisons) to account for multiple testing. Analyses of feeding modes were limited to passive and active suspension feeders, deposit feeders, scavengers, and predators; the grazers were not included because of low densities.

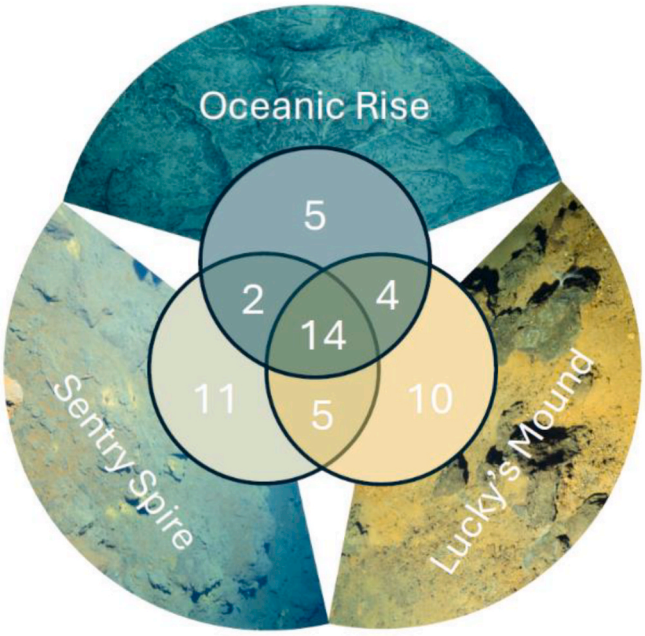

Fig. 4. Venn diagram of overlapping occurrence of morphotypes on inactive sulfides features Lucky's Mound, Sentry Spire, and the nearby oceanic rise. Background imagery shows typical substratum at each.

3. Results

3.1. Faunal patterns across sites

Faunal abundance, diversity, and community composition all varied notably across the three sites. A total of 2313 megafauna individuals was counted across 143 images, with pooled densities higher at Lucky's Mound (1.20 m^{-2}) and the Oceanic Rise (1.32 m^{-2}) than at Sentry Spire

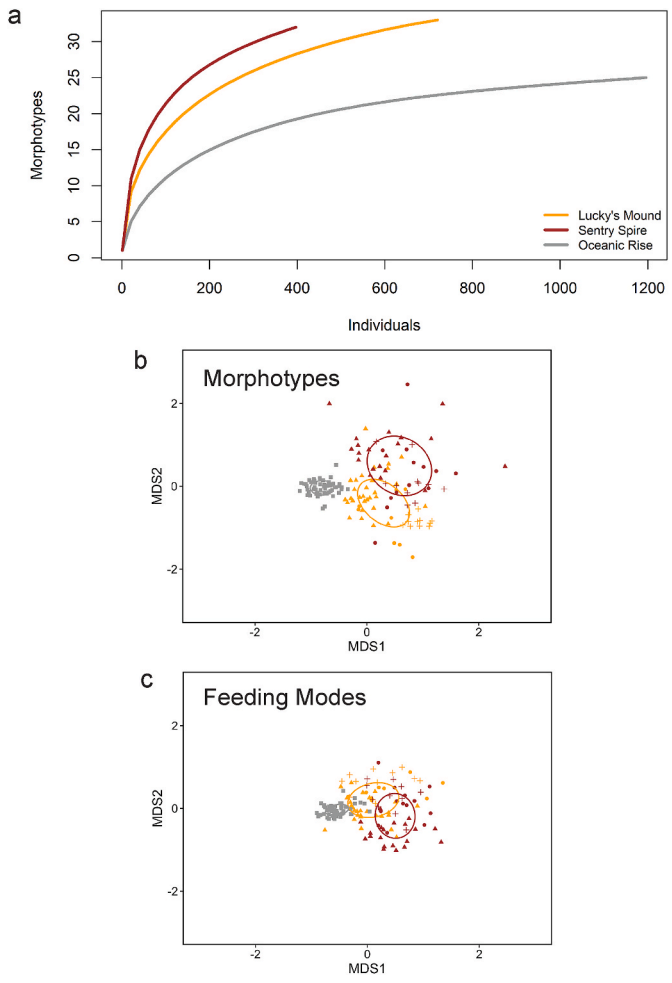

Fig. 5. Morphotype richness, morphotype composition, and feeding mode composition of megafaunal communities on inactive sulfide features (Lucky's Mound and Sentry Spire) and nearby flat seafloor (Oceanic Rise). (a) Morphotype accumulation as a function of number of individuals in the sample; (b) Non-metric multidimensional scaling (NMDS) ordination plots of community composition of morphotypes (Stress = 0.19); c) NMDS ordination plots of community composition of feeding modes (Stress = 0.18). In NMDS plots, habitat type is designated as spire (+), apron (·), base (·), and rise (·).

(0.35 m^{-2}). Fifty-one unique morphotypes of benthic megafauna were identified, of which only 14 were found at all three sites (Table 2). Abundant morphotypes on the inactive sulfides included xenophyophores (Foraminifera), a benthic ctenophore, a nematocarcinid shrimp, munidopsid crabs, brittle stars (Ophiurida) and crinoids (Antedonidae) (Fig. 3). Also notably abundant were a xenoturbellid-like organism on Lucky's Mound and a cladorhizid sponge on Sentry Spire. On the flat seafloor of the Oceanic Rise, the most abundant morphotypes were brittle stars, xenophyophores, and the benthic ctenophore. Although most of the morphotypes from the oceanic rise were also found on either or both inactive sulfides (20 of 25; 80%), fewer than half of morphotypes on the inactive sulfides also occurred on the rise (20 of 46; 43%) (Fig. 4). Ten morphotypes were recorded only from Lucky's Mound and 11 only from Sentry Spire. Only two of the morphotypes, the munidopsid and bythograeid crabs are recorded from active vents in this region.

Morphotype richness was distinctly higher at Sentry Spire and Lucky's Mound than on the nearby Oceanic Rise (Fig. 5a), and the morphotype rarefaction curves were not asymptotic, indicating that richness at these inactive sulfides is likely higher than observed here. Similarly, Shannon diversity indices were higher on the inactive sulfides (2.43 at Lucky's Mound; 2.74 at Sentry Spire) than on the Oceanic Rise (1.28), as were Pielou's evenness indices (0.70 at Lucky's Mound; 0.79 at Sentry Spire; 0.40 at Oceanic Rise).

Megafaunal composition differed across sites, especially between communities on the inactive sulfides and the oceanic rise where ordination clusters were nonoverlapping (Fig. 5b). Non-parametric, permutational multivariate analysis of variance (PERMANOVA) indicated a statistically significant difference in assemblages overall ($p < 0.001$), with significant pairwise differences between all sites (Lucky's-Rise $p < 0.001$; Sentry-Rise $p < 0.001$; Lucky's-Sentry $p < 0.05$). Feeding mode composition showed a clear distinction in assemblages between inactive sulfides and the oceanic rise but overlap between the two sulfide features (Fig. 5c). PERMANOVA indicated statistically significant difference in feeding mode compositions overall ($p < 0.001$), with significant pairwise differences between inactive sulfide sites and the oceanic rise (Lucky's-Rise: $p < 0.001$; Sentry-Rise: $p < 0.001$), but not between Lucky's Mound and Sentry Spire (Lucky's-Sentry: $p = 0.33$).

3.2. *Feeding mode patterns with elevation on sulfide features*

Densities of passive suspension-feeders and deposit feeders varied with elevation at both Lucky's Mound and Sentry Spire (Fig. 6; Supplementary Table 1). Kruskal-Wallis tests of all feeding modes indicated significant differences across habitat types, except for the predators. Passive suspension feeders were more abundant on the spires of both inactive sulfide features than at the base or on the oceanic rise, as detected by pairwise Dunn's tests. In contrast, deposit feeders tended to be less abundant on the apron or spire than at the rise or base, except at Sentry Spire where they were surprisingly abundant on the spire. The morphotype that drove this anomaly on Sentry Spire was the white xenophyophore, which was not found on the spire of Lucky's Mound but did occur further down on that feature and on the oceanic rise.

Active suspension-feeders and scavengers also showed interesting patterns across habitat types. Active suspension feeders tended to be more abundant on the spire and apron of both inactive sulfide features than the oceanic rise, but the patterns were not significant, and the densities at the base of Lucky's Mound were surprisingly high. The morphotype driving that anomaly was the benthic ctenophore, which also occurred at the base of Sentry Spire, but in lower numbers. Scavengers were markedly more abundant on the rise than on the inactive features but did not vary significantly across habitat type within a feature. Predators were relatively scarce and did not show distinct patterns with elevation on the features. Although scavengers and predators were separated into distinct categories for this study, it is likely that some of the larger crustacean scavengers (shrimp and crabs) may also feed opportunistically on live prey.

The remaining two feeding modes, grazer and unknown, each were represented by a single morphotype, "Polyplacophora, white chiton" and "*Xenoturbella*-like", respectively. The *Xenoturbella*-like morphotype was not assigned to a feeding mode because of the lack of available information on feeding traits for this taxon but also because of uncertainty in this taxonomic assignment. This morphotype was found only at Lucky's Mound, where it was the fifth most abundant megafaunal inhabitant and was notably more abundant on the spire and apron than at the base.

4. Discussion

The vertical distributions on inactive sulfide features of two main feeding modes, passive suspension-feeders and deposit feeders, generally corresponded to the expected hydrodynamically mediated supply of their respective food sources. Passive suspension feeders were expected to benefit from enhanced current-mediated particulate organic fluxes higher on the features, and deposit feeders were expected to benefit from enhanced particle deposition near the bases. Passive suspension feeders were more abundant on the spire for both features, and for the apron on

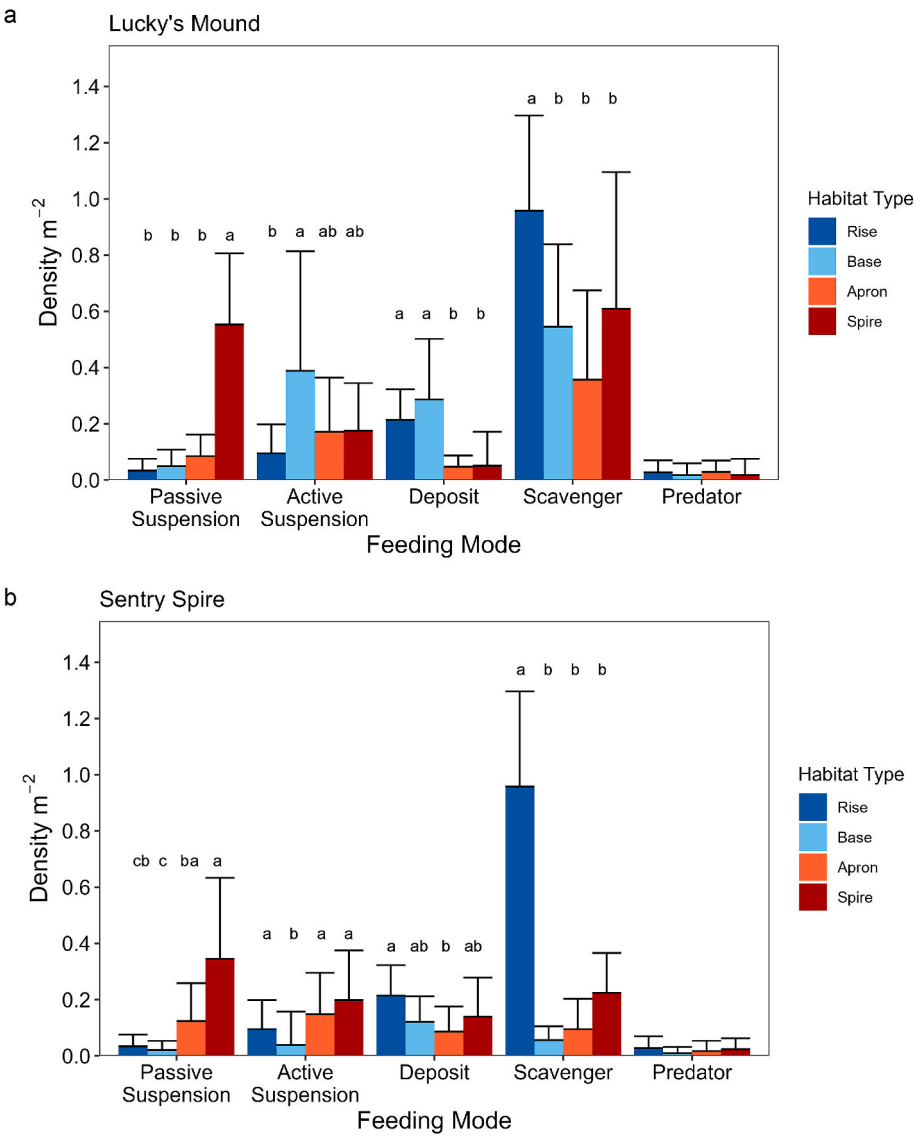

Fig. 6. Densities (mean and standard deviation) of individuals on Lucky's Mound (a) and Sentry Spire (b) in the five abundant feeding modes (Suspension-Passive, Suspension-Active, Deposit, Scavenger, Predator) across habitat types (Base, Apron, and Spire, with Oceanic Rise for comparison). On both features, variation across the habitat types was significant for all feeding modes except Predator (Kruskal-Wallis test, $p < 0.05$, with Bonferroni correction). Significant pairwise differences across the four habitat types (Dunn's test, $p < 0.05$ with Bonferroni correction) are designated with unshared letters at top of bars. Detail on sample sizes for each Habitat Type are in Supplementary Table 1.

Sentry Spire, than the other habitats. Deposit feeders tended to be less abundant on the spire and apron than at the base, except at Sentry Spire where white xenophyophores were abundant on the spire. Although we categorized these xenophyophores as deposit feeders, following Gooday et al. (1993), they may also suspension feed (Gooday et al., 2017). The patterns of passive suspension-feeders and deposit feeders support the suggestion that the physical structure of the features contributes to the uniqueness of assemblages there (Boschen et al., 2015), potentially by affecting the flux and deposition of particulate organic food (Johnson et al., 2013). The availability of hard substratum may also facilitate attachment of suspension feeders, but the distinct differences across spire, apron, and base, all having hard surfaces, indicate that substratum alone is not driving their densities.

The feeding-mode compositions of the two inactive sulfide features were similar but the morphotype compositions were distinctly different, with 46% of the morphotypes (21 of 46) detected on only one of the features. Many of these morphotypes were rare, and their detection could have been compromised by incomplete sampling or differences in camera altitude. However, the notable difference in community composition at the two features, including the presence of the distinct and abundant *Xenoturbella*-like morphotype only at Lucky's Mound, suggests that processes unrelated to feature morphology may be influencing the faunas. For example, the two features are small and thus may support only subsets of the biodiversity in the combined area of the many other inactive sulfide features in this region. The two features are located within 1 km of the active ridge axis and may receive different nutritional subsidies in the form of particulate chemosynthetically derived organic matter (Erickson et al., 2009) that influence megafaunal communities. Perhaps more likely is an influence of local microbial chemoautotrophy supported by the weathered sulfide rocks, as demonstrated on the East Pacific Rise by Sylvan et al. (2012) and Toner et al. (2013). Such a trophic influence, while difficult to detect in megafaunal communities, might become apparent in an investigation of smaller taxa that graze directly on microbes.

The distinct differences in morphotype composition and feeding modes that we observed within and between sulfide features, and from

nearby flat seafloor is generally consistent with previous studies from other regions. In the Edmond/Gauss vent field in the Indian Ocean, the animal assemblages observed on inactive sulfide deposits, 1.8 km away from active vents, were characterized by coral and sponge species, as distinct from those on nearby non-vent, peripheral, and active-vent substrata (Gerdes et al., 2019). In the Juan de Fuca region of the northeastern Pacific, the fauna of inactive sulfide features, at distances of 600–1000 m from active vents, was dominated by suspension feeders including corals, crinoids and rossellid sponges. This assemblage was similar to that observed on nearby basalt substrata and showed no influence of local chemoautotrophic influence, or subsidy from the nearby active vents (Neufeld et al., 2022). The fauna of inactive sulfide features that are very near active vents often overlap with vent-peripheral faunas (e.g., Marsh et al., 2012); making it difficult to determine what processes determine their composition. Hard-substratum communities not associated with vents, such as those on seamounts, also show differences in benthic faunal composition over small spatial scales and between nearby peaks, often associated with substratum type and topographic features, near-bottom currents, and microhabitat features (Shen et al., 2024).

Although our study region is not under consideration for deep-sea mining, our findings support a growing call to highlight biodiversity in conservation management plans for inactive sulfide deposits (Boschen et al., 2016). The new insights gained by examining vertical distributions of feeding modes contribute to a mechanistic explanation for how the physical structure of the features results in greater diversity of feeding options, particularly for suspension feeders. The variation in community composition between even very similar and closely spaced sulfide features points to the need for additional study of other influences, particularly those involving local microbial chemoautotrophic production, e.g., through stable isotopic analyses, and comparisons with other elevated, potentially basalt, features nearby.

CRediT authorship contribution statement

Michael J. Meneses: Writing – review & editing, Writing – original draft, Visualization, Methodology, Investigation, Formal analysis, Data curation, Conceptualization. **Stace E. Beaulieu:** Writing – review & editing, Visualization, Validation, Supervision, Resources, Project administration, Methodology, Investigation, Funding acquisition, Formal analysis, Data curation, Conceptualization. **Ayinde C. Best:** Writing – review & editing, Visualization, Methodology, Investigation, Formal analysis. **Lauren N. Dykman:** Writing – review & editing, Visualization, Methodology, Investigation, Formal analysis, Conceptualization. **Susan W. Mills:** Writing – review & editing, Visualization, Resources, Methodology, Investigation, Formal analysis. **Jyun-Nai Wu:** Writing – review & editing, Visualization, Methodology, Investigation, Formal analysis. **Lauren S. Mullineaux:** Writing – review & editing, Visualization, Supervision, Resources, Project administration, Methodology, Investigation, Funding acquisition, Formal analysis, Conceptualization.

Declaration of competing interest

The authors declare that they have no known competing financial interests or personal relationships that could have appeared to influence the work reported in this paper.

Data availability

Data included as Supplementary Table 1 and submitted to US BCODMO repository

Acknowledgments

We are grateful to the crews of the R/Vs *Atlantis* (AT42-21, AT50-06, AT50-20) and *Revelle* (RR2102), and the crews of DSVs *Sentry, Alvin*, and *Jason II*. Dan Fornari provided invaluable MISO imaging support for both cruises, and Karl Roberts and Andrew Sweetman assisted with imagery analysis for Cruise AT42-21. Discussions with Rose Jones, Jason Sylvan, Amanda Achberger, and Margaret Tivey were helpful in understanding the rocks and microbes at inactive sulfides. Shawn Arellano and Costa Vetriani generously allocated dive time to inactive sulfides exploration during the Biofilms project. Two anonymous reviewers provided insightful and helpful comments on the initial draft. Funding was provided from NSF OCE grants 1756339 to Sylvan, 1829773 to Mullineaux and Beaulieu, 1947735 to Mullineaux, 1949485 to Fornari, and 2152453 to Mullineaux and Beaulieu.

Appendix A. Supplementary data

Supplementary data to this article can be found online at https://doi.org/10.1016/j.marenvres.2024.106649.

References

Achberger, A.M., Jones, R., Jamieson, J., Holmes, C.P., Schubotz, F., Meyer, N.R., Dekas, A.E., Moriarty, S., Reeves, E.P., Manthey, A., Brunjes, J., Fornari, D.J., Tivey, B.M., Sylvan, J.B., 2024. Inactive hydrothermal vent microbial communities are important contributors to deep ocean primary productivity. Nat Microbiol 9, 657–668. https://doi.org/10.1038/s41564-024-01599-9.

Anderson, M.J., 2014. Permutational Multivariate Analysis of Variance (PERMANOVA). Wiley statsref: statistics reference online, pp. 1–15.

Boschen, R.E., Rowden, A.A., Clark, M.R., Gardner, J.P., 2013. Mining of deep-sea seafloor massive sulfides: a review of the deposits, their benthic communities, impacts from mining, regulatory frameworks and management strategies. Ocean Coast Manag. 84, 54–67.

Boschen, R.E., Rowden, A.A., Clark, M.R., Pallentin, A., Gardner, J.B.A., 2016. Seafloor massive sulfide deposits support unique megafaunal assemblages: implications for seabed mining and conservation. Mar. Environ. Res. 115, 78–88. https://doi.org/10.1016/j.marenvres.2016.02.005.

Boschen, R.E., Rowden, A.A., Clark, M.R., Barton, S.J., Pallentin, A., Gardner, J.P., 2015. Megabenthic assemblage structure on three New Zealand seamounts: implications for seafloor massive sulfide mining. Mar. Ecol. Prog. Ser. 523, 1–14.

Boschen-Rose, R.E., Clark, M.R., Rowden, A.A., Gardner, J.P., 2021. Assessing the ecological risk to deep-sea megafaunal assemblages from seafloor massive sulfide mining using a functional traits sensitivity approach. Ocean Coast Manag. 210, 105656.

Bray, J.R., Curtis, J.T., 1957. An ordination of the upland forest communities of southern Wisconsin. Ecol. Monogr. 27 (4), 326–349.

Cadotte, M.W., Carscadden, K., Mirotchnick, N., 2011. Beyond species: functional diversity and the maintenance of ecological processes and services. J. Appl. Ecol. 48 (5), 1079–1087.

Chapman, A.S., Beaulieu, S.E., Colaço, A., Gebruk, A.V., Hilario, A., Kihara, T.C., Bates, A.E., 2019. sFDvent: a global trait database for deep-sea hydrothermal-vent fauna. Global Ecol. Biogeogr. 28 (11), 1538–1551.

Chen, C., Zhou, Y., Watanabe, H.K., Zhang, R., Wang, C., 2021. Neolepetopsid true limpets (Gastropoda: patellogastropoda) from Indian Ocean hot vents shed light on relationships among genera. Zool. J. Linn. Soc. 1–21. http://zoobank.org/urn:lsid:zoobank.org:pub:6334CD15-D490-496F-802A-F162B4FF8A21.

Chen, C., Li, Y., Sun, J., Beaulieu, S.E., Mullineaux, L.S., 2024. Two new melanodrymiid snails from the East Pacific Rise indicate the potential role of inactive vents as evolutionary stepping-stones. Syst. Biodivers. 22 (1) https://doi.org/10.1080/14772000.2023.2294014.

Desbruyères, D., Segonzac, M., Bright, M., 2006. Handbook of deep-sea hydrothermal vent fauna. Denisia 544 second ed.

Dunn, O.J., 1961. Multiple comparisons among means. J. Am. Stat. Assoc. 56 (293), 52–64.

Durden, J.M., Schoening, T., Althaus, F., Friedman, A., Garci, R., Glover, A.G., et al., 2016. Perspectives in visual imaging for marine biology and ecology: from acquisition to understanding. In: Oceanography and Marine Biology. CRC Press, pp. 9–80.

Dykman, L.N., Beaulieu, S.E., Mills, S.W., Solow, A.R., Mullineaux, L.S., 2021. Functional traits provide new insight into recovery and succession at deep-sea hydrothermal vents. Ecology 102 (8), e03418.

Erickson, K.L., Macko, S.A., Van Dover, C.L., 2009. Evidence for a chemoautotrophically based food web at inactive hydrothermal vents (Manus Basin). Deep Sea Res. Part II Top. Stud. Oceanogr. 56 (19–20), 1577–1585.

Fornari, D.J., Von, Damm K., Bryce, J.G., Cowen, J.P., Ferrini, V., Fundis, A., et al., 2012. The East Pacific Rise between 9°N and 10°N: twenty-five years of integrated, multidisciplinary oceanic spreading center studies. Oceanography 25 (1), 18–43. https://doi.org/10.5670/oceanog.2012.02.

Gerdes, K.H., Arbizu, P.M., Schwentner, M., Freitag, R., Schwarz-Schampera, U., Brandt, A., Kihara, T.C., 2019. Megabenthic assemblages at the southern Central Indian Ridge–spatial segregation of inactive hydrothermal vents from active-, periphery-and non-vent sites. Mar. Environ. Res. 151, 104776.

Gerdes, K.H., Kihara, T.C., Arbizu, P.M., Molodtsova, T., 2021. Megafauna of the German exploration license area for seafloor massive sulphides along the Central and South East Indian Ridge (Indian Ocean). Biodivers. Data J. https://doi.org/10.3897/BDJ.9.e69955.

Goldfarb, M.S., Converse, D.R., Holland, H.D., Edmond, J.M., 1983. The genesis of hot spring deposits on the East Pacific rise, 21°N. Econ. Geol. Monogr. 5, 184–197.

Gooday, A.J., Bett, B.J., Pratt, D.N., 1993. Direct observation of episodic growth in an abyssal xenophyophore (Protista). Deep-Sea Res. I 40, 2131–2143. https://doi.org/10.1016/0967-0637(93)90094-J.

Gooday, A.J., Holzmann, M., Caulle, C., Goineau, A., Kamenskaya, O., Weber, A.A.-T., Pawlowski, J., 2017. Giant protists (xenophyophores, Foraminifera) are exceptionally diverse in parts of the abyssal eastern Pacific licensed for polymetallic nodule exploration. Biol. Conserv. 207, 106–116. https://doi.org/10.1016/j.biocon.2017.01.006.

Hannington, M.D., Jamieson, J.W., Monecke, T., Petersen, S., 2010. Modern seafloor massive sulfides and base metal resources: toward an estimate of global seafloor massive sulfide potential. The Challenge of Finding New Mineral Resources: Global Metallogeny, Innovative Exploration, and New Discoveries 317–338. https://doi.org/10.5382/SP.15.2.001.

Horton, T., Marsh, L., Bett, B.J., Gates, A.R., Jones, D.O., Benoist, N., et al., 2021. Recommendations for the standardisation of open taxonomic nomenclature for image-based identifications. Front. Mar. Sci. 8, 62. https://doi.org/10.3389/fmars.2021.620702.

Jamieson, J.W., Gartman, A., 2020. Defining active, inactive, and extinct seafloor massive sulfide deposits. Mar. Pol. 117, 103926 https://doi.org/10.1016/j.marpol.2020.103926.

Johnson, M.P., White, M., Wilson, A., Würzberg, L., Schwabe, E., Folch, H., Allcock, A.L., 2013. A vertical wall dominated by *Acesta excavata* and *Neopycnodonte zibrowii*, part of an undersampled group of deep-sea habitats. PLoS One 8, e79917.

Kassambara, A., 2023. Rstatix: pipe-friendly framework for basic statistical tests. R package version 0.7.2. https://CRAN.R-project.org/package=rstatix.

Kato, S., Takano, Y., Kakegawa, T., et al., 2010. Biogeography and biodiversity in sulfide structures of active and inactive vents at deep-sea hydrothermal fields of the Southern Mariana Trough. Appl. Environ. Microbiol. 76 (9), 2968–2979. https://doi.org/10.1128/AEM.00478-10.

Kruskal, W.H., Wallis, W.A., 1952. Use of ranks in one-criterion variance analysis. J. Am. Stat. Assoc. 47, 583–621. https://doi.org/10.1080/01621459.1952.10483441.

Kruskal, J.B., 1964. Nonmetric multidimensional scaling: a numerical method. Psychometrika 29 (2), 115–129.

Leichter, J.J., Witman, J.D., 1997. Water flow over subtidal rock walls: relation to distributions and growth rates of sessile suspension feeders in the Gulf of Maine. J. Exp. Mar. Biol. Ecol. 209, 293–307.

MarLIN, 2006. Biotic - biological traits information Catalogue. In: Marine Life Information Network. Plymouth: Marine Biological Association of the United Kingdom [2024-04-16] Available from. www.marlin.ac.uk/biotic.

Marsh, L., Copley, J.T., Huvenne, V.A.I., Linse, K., Reid, W.D.K., et al., 2012. Microdistribution of faunal assemblages at Deep-Sea hydrothermal vents in the southern ocean. PLoS One 7 (10), e48348. https://doi.org/10.1371/journal.pone.0048348.

McDermott, J.M., Parnell-Turner, R., Barreyre, T., et al., 2022. Discovery of active off-axis hydrothermal vents at 9°54′N East Pacific rise. Proc. Natl. Acad. Sci. USA 119 (30), e2205602119.

McLean, J.H., 1990. Neolepetopsidae, a new docoglossate limpet family from hydrothermal vents and its relevance to patellogastropod evolution. J. Zool. 222 (3), 485–528.

Morim, T., Henriques, S., Vasconcelos, R., Dolbeth, M., 2023. A roadmap to define and select aquatic biological traits at different scales of analysis. Sci. Rep. 13, 22947 https://doi.org/10.1038/s41598-023-50146-9.

Mouillot, D., Graham, N.A.J., Villéger, S., Mason, N.W.H., Bellwood, D.R., 2013. A functional approach reveals community responses to disturbances. Trends Ecol. Evol. 28 (3), 167–177. https://doi.org/10.1016/j.tree.2012.10.004.

Neufeld, M.B., Metaxas, A., Jamieson, J.W., 2022. Non-vent megafaunal communities on the Endeavour and Middle Valley segments of the Juan de Fuca Ridge, Northeast Pacific Ocean. Front. Mar. Sci. 804 https://doi.org/10.3389/fmars.2022.849976.

NOAA, 2019. Ocean exploration benthic deepwater animal identification Guide v3. Available from. http://oceanexplorer.noaa.gov/okeanos/animal_guide/animal_guide.html.

Oksanen, J., Simpson, G., Blanchet, F., Kindt, R., Legendre, P., Minchin, P., O'Hara, R., Solymos, P., Stevens, M., Szoecs, E., Wagner, H., Barbour, M., Bedward, M., Bolker, B., Borcard, D., Carvalho, G., Chirico, M., De Caceres, M., Durand, S., Evangelista, H., FitzJohn, R., Friendly, M., Furneaux, B., Hannigan, G., Hill, M., Lahti, L., McGlinn, D., Ouellette, M., Ribeiro Cunha, E., Smith, T., Stier, A., Ter Braak, C., Weedon, J., 2022. Vegan: community ecology package. R package version 2.6-4. https://CRAN.R-project.org/package=vegan.

Orcutt, B.N., Bradley, J.A., Brazelton, W.J., Pachiadaki, M., 2020. Impacts of deep-sea mining on microbial ecosystem services. Limnol. Oceanogr. 65 (7), 1489–1510. https://doi.org/10.1002/lno.11403.

Parnell-Turner, R., Fornari, D., McDermott, J., Barreyre, T., Wu, J.N., 2021. Processed bathymetric data (netCDF grid) from 9°50'N, East Pacific Rise, acquired in 2018, 2019 and 2021 during AUV Sentry near-bottom dives. IEDA. https://doi.org/10.26022/IEDA/330373.

Pettibone, M.H., 1984. Two new species of *lepidonotopodium* (polychaeta: polynoidae: lepidonotopodinae) from hydrothermal vents off the galapagos and East Pacific rise at 21°N. Proc. Biol. Soc. Wash. 97 (4), 849–863.

Pielou, E.C., 1966. The measurement of diversity in different types of biological collections. J. Theor. Biol. 13, 131–144. https://doi.org/10.1016/0022-5193(66)90013-0.

R Core Team, 2023. R: A Language and Environment for Statistical Computing. R Foundation for Statistical Computing, Vienna, Austria. URL. https://www.R-project.org/.

Schneider, C.A., Rasband, W.S., Eliceiri, K.W., 2012. NIH Image to ImageJ: 25 years of image analysis. Nat. Methods 9 (7), 671–675.

Shannon, C.E., 1948. A mathematical theory of communication. Bell System Tech. J. 27 (3), 379–423.

Shen, C., Yan, R., Lu, B., Li, Z., Zhang, R., Zhang, D., Wang, C., 2024. Dissimilarity of megabenthic community structure between deep-water seamounts with cobalt-rich crusts: case study in the northwestern Pacific Ocean. Sci. Total Environ. 945, 173914 https://doi.org/10.1016/j.scitotenv.2024.173914.

Simon-Lledó, E., Amon, D.J., Bribiesca-Contreras, G., et al., 2023. Abyssal Pacific Seafloor Megafauna Atlas (1.0). Zenodo. https://doi.org/10.5281/zenodo.8172728.

Sylvan, J.B., Toner, B.M., Edwards, K.J., 2012. Life and death of deep-sea vents: bacterial diversity and ecosystem succession on inactive hydrothermal sulfides. mBio 3 (1), e00279, 11.

Tivey, M.K., 2007. Generation of seafloor hydrothermal vent fluids and associated mineral deposits. Oceanography 20 (SPL.ISS. 1), 50–65. https://doi.org/10.5670/oceanog.2007.80.

Toner, B.M., Lesniewski, R.A., Marlow, J.J., et al., 2013. Mineralogy drives bacterial biogeography of hydrothermally inactive seafloor sulfide deposits. Geomicrobiol. J. 30 (4), 313–326. https://doi.org/10.1080/01490451.2012.688925.

Van Dover, C.L., 2019. Inactive sulfide ecosystems in the deep sea: a review. Front. Mar. Sci. 6, 461 gf6qvb.

Wessel, P., Luis, J.F., Uieda, L., Scharroo, R., Wobbe, F., Smith, W.H.F., Tian, D., 2019. The generic mapping tools version 6. G-cubed 20 (11), 5556–5564. https://doi.org/10.1029/2019GC008515.

WoRMS Editorial Board, 2022. World Register of Marine Species. Available from. http://www.marinespecies.orgatVLIZ. (Accessed 3 April 2022). https://doi.org/10.14284/170.

Wu, J.N., Parnell-Turner, Fornari, D.J., McDermott, J.M., 2022. Extent and volume of lava flows erupted at 9°50′N, East Pacific Rise in 2005–2006 from autonomous underwater vehicle surveys. G-cubed 23 (3), e2021GC010213.

Zhou, Y., Chen, C., Sun, Y., Watanabe, H.K., Zhang, R., Wang, C., 2019. *Amphisamytha* (Annelida: ampharetidae) from Indian ocean hydrothermal vents: biogeographic implications. Deep-Sea Res. I 154. https://doi.org/10.1016/j.dsr.2019.103148.